Charged particle correlations in pseudorapidity bins in minimum bias pp collisions at $\sqrt{s} = 2.76$ TeV

Jakub Kremer Piotr Janus
AGH University of Science and Technology, Kraków

September 4, 2013

Abstract

This report is the summary of our work during the DESY Summer Student Programme 2013. It describes measurement of long range correlations of charged particles in data from pp collisions collected by the ATLAS experiment at a center of mass energy $\sqrt{s} = 2.76$ TeV. The correlations are compared to those predicted by hydrodynamical models of the collision which contain one or two particle-emitting sources. First preparations for a similar analysis with high multiplicity data are also presented.

Contents

1 Introduction and theory

Studies of correlations between particles produced in high energy collisions may help to understand partonic interactions leading to hadronization in a more complete way. Long range correlations are very useful, since they provide understanding of the early stages of a collision. Such correlations cannot appear in the later stages of a collision, because the system has to be small enough to let them extend through itself.
Recently a general method has been proposed [1] to study correlations using several bins in rapidity. This method is intended to provide a statistical test for hydrodynamical models which describe the longitudinal expansion of the system in the early stages of a collision. In particular, it should give information about the number of independent particle-emitting sources created in the collision. Assuming that the particles from each source are distributed randomly (i.e. it does not influence long range correlations), the generating function for the particle distribution in B bins takes the form [2]:

$$\Phi\left(z_1,...,z_B\right) \equiv \sum_{n_1+...+n_B=n} P\left(n_1,...,n_B\right) z_1^{n_1}...\, z_B^{n_B} = \prod_{i=1}^{N} \phi_i\left(p_{1i}z_1 + ... + p_{Bi}z_B\right) \tag{1}$$

where ϕ_i is the generating function describing the multiplicity distribution of particles emitted by the i-th source. The parameters p_{ki} are probabilities of the multinomial distribution $P\left(n_1,...,n_B;n\right)$ according to which the i-th source sends particles to the k-th bin. It is obvious that $p_{1i} + ... + p_{Bi} = 1$ for each i. It is worth mentioning that the generating functions ϕ_i do not have to be all different.
In this analysis factorial moments are used, where a factorial moment of rank r ($r = i_1 + ... + i_B$) is defined as:

$$F_{i_1,...,i_B} \equiv \left\langle \prod_{j=1}^{B} \frac{n_j!}{(n_j - i_j)!} \right\rangle = \frac{\partial^r \Phi(z_1,...,z_B)}{\partial z_1^{i_1}...\,\partial z_B^{i_B}} \tag{2}$$

with derivatives taken at $z_1 = ... = z_B = 1$.
One can also define moments of the total multiplicity distribution which are given by:

$$F_i \equiv \left\langle \frac{n!}{(n-i)!} \right\rangle = \left. \frac{\partial^i \Phi(z)}{\partial z^i} \right|_{z=1} \tag{3}$$

In the case of three bins, L - left, R - right and C - central, one gets $p_L + p_R + p_C = 1$. It is easy to show that the expressions for 19 measurable factorial moments up to rank 3 can be expressed in terms of 5 independent parameters (two of the probabilities and the first three moments of the total multiplicity distribution) [3]:

$$\begin{array}{lll}
F_{100} = p_L F_1, & F_{010} = p_C F_1 & F_{001} = p_R F_1 \\
F_{200} = p_L^2 F_2, & F_{020} = p_C^2 F_2 & F_{002} = p_R^2 F_2 \\
F_{110} = p_L p_C F_2, & F_{101} = p_L p_R F_2 & F_{011} = p_C p_R F_2 \\
F_{210} = p_L^2 p_C F_3, & & F_{012} = p_C p_R^2 F_3 \\
F_{201} = p_L^2 p_R F_3 & & F_{102} = p_L p_R^2 F_3 \\
F_{120} = p_L p_C^2 F_3, & F_{111} = p_L p_C p_R F_3 & F_{021} = p_C^2 p_R F_3 \\
F_{300} = p_L^3 F_3, & F_{030} = p_C^3 F_3 & F_{003} = p_R^3 F_3
\end{array} \tag{4}$$

where

$$F_{i_L,i_C,i_R} = \left\langle \frac{n_L!}{(n_L - i_L)!} \frac{n_C!}{(n_C - i_C)!} \frac{n_R!}{(n_R - i_R)!} \right\rangle \tag{5}$$

and n_b is the number of particles in bin b.
In the case of two independent sources the number of measurable factorial moments up to rank 3 amounts to 19 for three bins. The numbers of parameters in the model is 10. The formulas for the factorial moments read:

$$\begin{aligned}
F_{100} &= p_{L1}F_1^{(1)} + p_{L2}F_1^{(2)} \\
F_{010} &= p_{C1}F_1^{(1)} + p_{C2}F_1^{(2)} \\
F_{001} &= p_{R1}F_1^{(1)} + p_{R2}F_1^{(2)} \\
F_{110} &= p_{L1}p_{C1}F_2^{(1)} + p_{L2}p_{C2}F_2^{(2)} + (p_{L1}p_{C2} + p_{L2}p_{C1})F_1^{(1)}F_1^{(2)} \\
F_{101} &= p_{L1}p_{R1}F_2^{(1)} + p_{L2}p_{R2}F_2^{(2)} + (p_{L1}p_{R2} + p_{L2}p_{R1})F_1^{(1)}F_1^{(2)} \\
F_{011} &= p_{C1}p_{R1}F_2^{(1)} + p_{C2}p_{R2}F_2^{(2)} + (p_{C1}p_{R2} + p_{C2}p_{R1})F_1^{(1)}F_1^{(2)} \\
F_{200} &= p_{L1}^2F_2^{(1)} + p_{L2}^2F_2^{(2)} + 2p_{L1}p_{L2}F_1^{(1)}F_1^{(2)} \\
F_{020} &= p_{C1}^2F_2^{(1)} + p_{C2}^2F_2^{(2)} + 2p_{C1}p_{C2}F_1^{(1)}F_1^{(2)} \\
F_{002} &= p_{R1}^2F_2^{(1)} + p_{R2}^2F_2^{(2)} + 2p_{R1}p_{R2}F_1^{(1)}F_1^{(2)} \\
F_{111} &= p_{L1}p_{C1}p_{R1}F_3^{(1)} + p_{L2}p_{C2}p_{R2}F_3^{(2)} \\
&\quad + (p_{L2}p_{C1}p_{R1} + p_{L1}p_{C2}p_{R1} + p_{L1}p_{C1}p_{R2})F_2^{(1)}F_1^{(2)} \\
&\quad + (p_{L1}p_{C2}p_{R2} + p_{L2}p_{C1}p_{R2} + p_{L2}p_{C2}p_{R1})F_1^{(1)}F_2^{(2)} \\
F_{210} &= p_{L1}^2p_{C1}F_3^{(1)} + p_{L2}^2p_{C2}F_3^{(2)} \\
&\quad + (p_{L1}^2p_{C2} + 2p_{L1}p_{L2}p_{C1})F_2^{(1)}F_1^{(2)} \\
&\quad + (p_{L2}^2p_{C1} + 2p_{L1}p_{L2}p_{C2})F_1^{(1)}F_2^{(2)} \\
F_{012} &= p_{C1}p_{R1}^2F_3^{(1)} + p_{C2}p_{R2}^2F_3^{(2)} \\
&\quad + (p_{C2}p_{R1}^2 + 2p_{C1}p_{R1}p_{R2})F_2^{(1)}F_1^{(2)} \\
&\quad + (p_{C1}p_{R2}^2 + 2p_{R1}p_{R2}p_{C2})F_1^{(1)}F_2^{(2)} \\
F_{201} &= p_{L1}^2p_{R1}F_3^{(1)} + p_{L2}^2p_{R2}F_3^{(2)} \\
&\quad + (p_{L1}^2p_{R2} + 2p_{L1}p_{L2}p_{R1})F_2^{(1)}F_1^{(2)} \\
&\quad + (p_{L2}^2p_{R1} + 2p_{L1}p_{L2}p_{R2})F_1^{(1)}F_2^{(2)} \\
F_{102} &= p_{L1}p_{R1}^2F_3^{(1)} + p_{L2}p_{R2}^2F_3^{(2)} \\
&\quad + (p_{L2}p_{R1}^2 + 2p_{L1}p_{R1}p_{R2})F_2^{(1)}F_1^{(2)} \\
&\quad + (p_{L1}p_{R2}^2 + 2p_{R1}p_{R2}p_{L2})F_1^{(1)}F_2^{(2)} \\
F_{021} &= p_{C1}^2p_{R1}F_3^{(1)} + p_{C2}^2p_{R2}F_3^{(2)} \\
&\quad + (p_{C1}^2p_{R2} + 2p_{C1}p_{C2}p_{R1})F_2^{(1)}F_1^{(2)} \\
&\quad + (p_{C2}^2p_{R1} + 2p_{C1}p_{C2}p_{R2})F_1^{(1)}F_2^{(2)}
\end{aligned}$$

$$
\begin{aligned}
F_{120} &= p_{L1}p_{C1}^2F_3^{(1)} + p_{L2}p_{C2}^2F_3^{(2)} \\
&\quad +(p_{L2}p_{C1}^2 + 2p_{L1}p_{C1}p_{C2})F_2^{(1)}F_1^{(2)} \\
&\quad +(p_{L1}p_{C2}^2 + 2p_{C1}p_{C2}p_{L2})F_1^{(1)}F_2^{(2)} \\
F_{300} &= p_{L1}^3F_3^{(1)} + p_{L2}^3F_3^{(2)} + 3p_{L1}^2p_{L2}F_2^{(1)}F_1^{(2)} + 3p_{L1}p_{L2}^2F_1^{(1)}F_2^{(2)} \\
F_{030} &= p_{C1}^3F_3^{(1)} + p_{C2}^3F_3^{(2)} + 3p_{C1}p_{C2}^2F_1^{(1)}F_2^{(2)} + 3p_{C1}^2p_{C2}F_2^{(1)}F_1^{(2)} \\
F_{003} &= p_{R1}^3F_3^{(1)} + p_{R2}^3F_3^{(2)} + 3p_{R1}p_{R2}^2F_1^{(1)}F_2^{(2)} + 3p_{R1}^2p_{R2}F_2^{(1)}F_1^{(2)}
\end{aligned} \tag{6}
$$

In this analysis a measurement of multiplicity correlations in three bins in pseudorapidity is presented for pp collisions at a center of mass energy $\sqrt{s} = 2.76$ TeV. For the measurement a central bin and two other symmetrically placed bins around 0 are chosen. The width of each bin is 0.5 pseudorapidity units and the distance between the centres of the left and right bin varies from 1.5 to 3.5 units. The obtained factorial moments are then used to test the validity of models with either one or two sources. In the first case some of the measured factorial moments are used to calculate the parameters of the model. Then one can express the other factorial moments through these parameters and compare them to the measured values. However, for the two source model a simultaneous fit of 10 parameters to 19 equations has to be done.

2 Event selection

The dataset used in this analysis was collected in 2011 during run 178229 at the ATLAS detector. It contains data from pp collisions with reduced pileup. Minimum bias events are selected according to the following requirements:

- Minimum Bias trigger - EF_mbMBTS_2_NoAlg which requires at least two hits in the MBTS detectors irrespectively of their side,
- Primary Vertex and at least two tracks pointing to this vertex,
- At least one good reconstructed track[1],
- Requirement on z coordinate of the primary vertex: $|v_z| < 100$ mm.

Table 1 shows the number of events passing the subsequent selection cuts.

Cuts	Events [millions]
Total after trigger	4.5
After good vertex	3.8
After good tracks	3.7
$\lvert v_z\rvert < 100$ mm	3.2

Table 1: Cut flow of minimum bias event selection.

[1]Definition of good tracks is given in the next section

3 Track selection

In this analysis ATLAS Standard Minimum Bias (MB2.0) cuts [4] are used for selecting good reconstructed tracks. The additional requirements on d_0 and $z_0 \sin(\theta)$ significances help to remove tracks which are incorrectly reconstructed or come from secondary particles. Table 2 defines the requirements for tracks which are considered to be correctly reconstructed.

p_T	> 0.1 GeV
$\lvert\eta\rvert$	< 2.5
Number of Pixel hits	≥ 1
Number of SCT hits	≥ 2 for 0.1 GeV $< p_T <$ 0.2 GeV
Number of SCT hits	≥ 4 for 0.2 GeV $< p_T <$ 0.3 GeV
Number of SCT hits	≥ 6 for $p_T > 0.3$ GeV
d_0^{PV} significance	≤ 3
$z_0^{PV} \sin(\theta)$ significance	≤ 3
$\lvert d_0^{PV} \rvert$	≤ 1.5 mm
$\lvert z_0^{PV} \sin(\theta) \rvert$	≤ 1.5 mm
Number of B-Layer hits (if expected)	≥ 1
TMath::Prob(χ^2,DoF)	≥ 0.01 for $p_T > 10$ GeV

Table 2: Cuts defining good tracks.

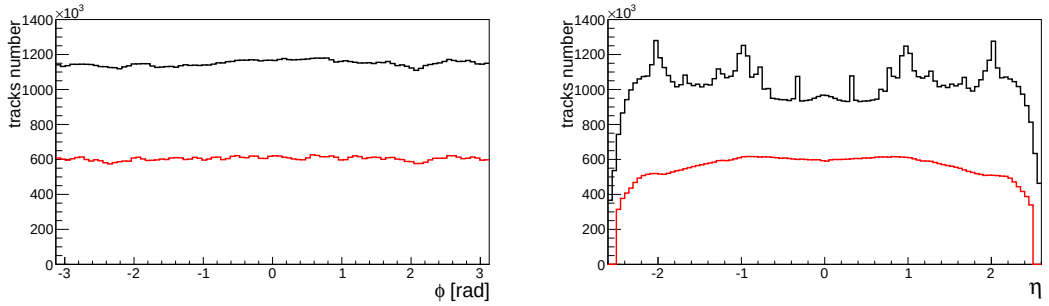

Figure 1: Distributions of ϕ (left) and η (right). Black histograms show all tracks while the red histograms show only tracks passing the selection cuts. The track selection does not change the ϕ distribution and removes peaks from the η distribution.

4 Tracking efficiency, fakes and secondaries ratios

4.1 Track reconstruction efficiency

The tracking efficiency for this analysis is obtained using a Monte Carlo sample from Pythia 6 which contains 8.8 millions of events. It is calculated in bins of η and p_T using the information about generated particles and reconstructed tracks matching to these particles. Reconstructed tracks are required to pass the selection cuts defined in

Section 3, while the following conditions are used to select primary particles from the generator level:

- Particle has to be stable and coming from primary vertex which is given by a barcode value between 0 and 200000,
- Particle has to be charged,
- Requirement on particle pseudorapidity $|\eta| < 2.5$,
- Transverse momentum requirement $p_T > 100$ MeV.

With these requirements the tracking efficiency can be defined as:

$$eff = \frac{N^{reco}_{matched}}{N_{truth}} \tag{7}$$

where $N^{reco}_{matched}$ is the number of good reconstructed tracks matched with a particle from the truth (generator) level and N_{truth} is the number of all generated particles.

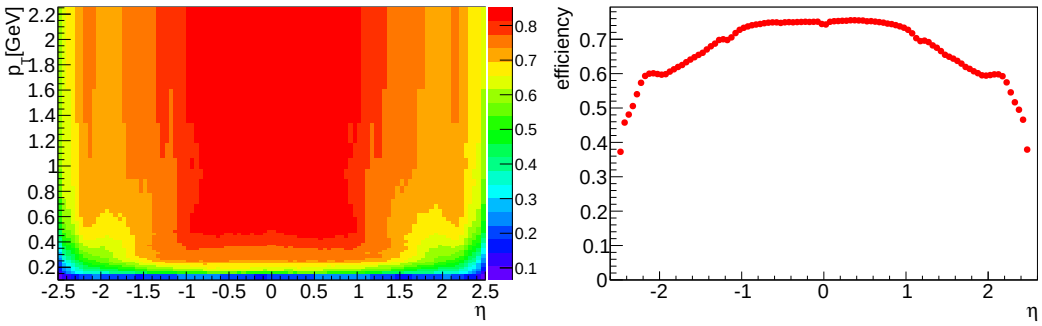

Figure 2: Track reconstruction efficiency as a function of η and p_T (left) and as a projection on the η axis (right).

4.2 Fakes fraction

The tracking efficiency calculated according to (7) does not include the effect of incorrectly reconstructed tracks called fakes. In order to be able to correct for this contribution the fakes ratio is defined as:

$$f = \frac{N^{reco}_{unmatched}}{N^{reco}} \tag{8}$$

where $N^{reco}_{unmatched}$ is the number of reconstructed tracks which do not have a matching particle at the truth level and N^{reco} is the number of all reconstructed tracks.

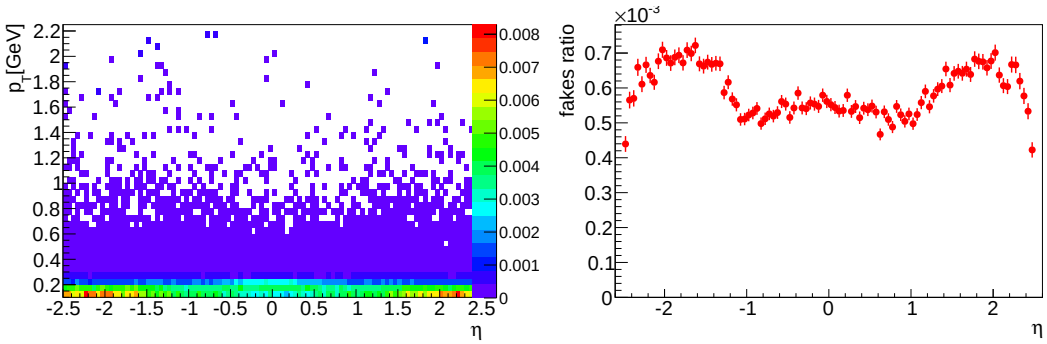

Figure 3: Fakes ratio as a function of η and p_T (left) and as a projection on the η axis (right).

4.3 Secondaries fraction

Secondary particles created in decays of primary particles or in their interaction with the detector material also contribute to the overall tracking efficiency. The secondaries ratio is defined as:

$$s = \frac{N^{reco,sec}_{matched}}{N^{reco}} \tag{9}$$

where $N^{reco,sec}_{matched}$ is the number of reconstructed tracks which match a secondary particle from the truth level and N^{reco} is the number of all reconstructed tracks. The identification of secondary particles is based on their barcode which is higher than 200000.

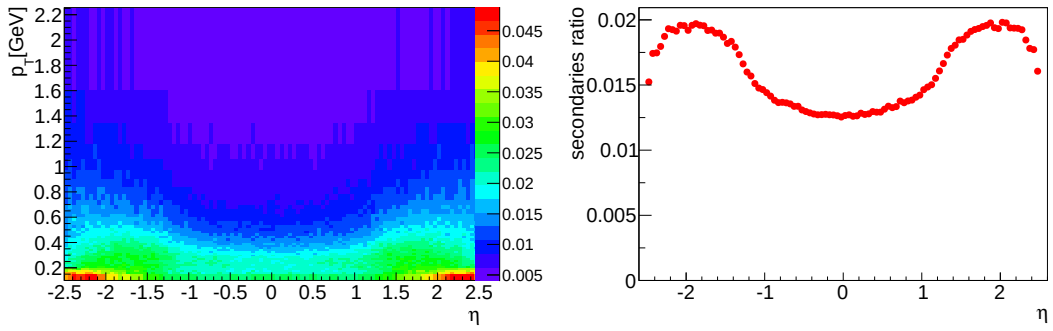

Figure 4: Secondaries ratio as a function of η and p_T (left) and as a projection on the η axis (right).

5 Corrections

5.1 The HBOM procedure

For correcting inefficiencies of track reconstruction the Hit Backspace Once More (HBOM) procedure [5] is chosen. This method relies only on the correct definition of the tracking efficiency. It implies that random removal of tracks from the sample can imitate detector inefficiencies.
The observable, that has to be corrected, is first measured using all reconstructed tracks

which pass the selection cuts. This step is called the 0th iteration of the procedure. Then some of the tracks are removed by comparing for each track the tracking efficiency to a random number r generated uniformly between 0 and 1. Important is that one needs to use the tracking efficiency eff corrected by the fakes and secondaries ratios (f and s respectively):

$$\frac{eff}{(1-f)(1-s)} > r \tag{10}$$

Tracks which do not satisfy condition (10) are rejected from the sample. After that, the observable is calculated again which defines one iteration of the HBOM method. Further iterations follow the same principle. With several iterations carried out, an exponential or polynomial can be fitted to the distribution of the observable as a function of the iteration number. An extrapolation of the fitted function to the iteration -1 can then estimate the true value of the observable. Figure 5 is showing an example of the HBOM method applied to a factorial moment.

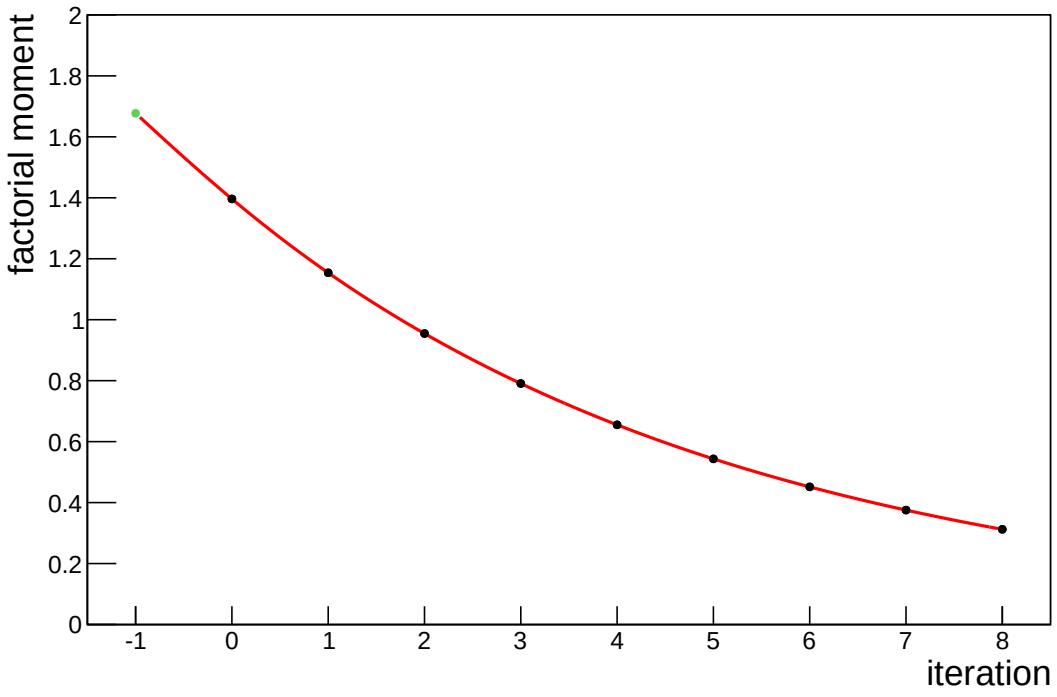

Figure 5: Black points mark the values of a factorial moment after subsequent iterations of the HBOM procedure. The green point is the true value obtained by extrapolating a fitted function.

5.2 Validation of the HBOM method

For testing the HBOM procedure, the Monte Carlo sample is divided into two parts. The first one is used to calculate tracking efficiency, secondaries and fakes ratios, while the second one to measure factorial moments. The test is carried out by comparing factorial moments obtained from the generator level and from unfolding the reconstructed level using various fitting functions and numbers of iterations. On the truth level only particles

which satisfy the requirements listed in Section 4.1. are counted, while tracks from the reconstructed level have to pass the selection cuts described in Section 3.
Factorial moments are measured in three bins with varying distance between the centres of the left and right bin as shown in Table 3. The central bin is the same in each case.

Left	Central	Right
$-1 < \eta < -0.5$	$-0.25 < \eta < 0.25$	$0.5 < \eta < 1$
$-1.5 < \eta < -1$	$-0.25 < \eta < 0.25$	$1 < \eta < 1.5$
$-2 < \eta < -1.5$	$-0.25 < \eta < 0.25$	$1.5 < \eta < 2$

Table 3: Pseudorapidity intervals used to validate the HBOM method and for measurement.

To validate the HBOM method different polynomials and exponentials are tested with a varying number of iterations. In this report we present the comparison of a 6^{th} degree polynomial and the exponential function e^{ax^2+bx+c}. These functions give the best results when the number of iterations is set to 7. For further iterations the distribution of factorial moments flattens which affects strongly the fitting function and therefore the unfolded true values.

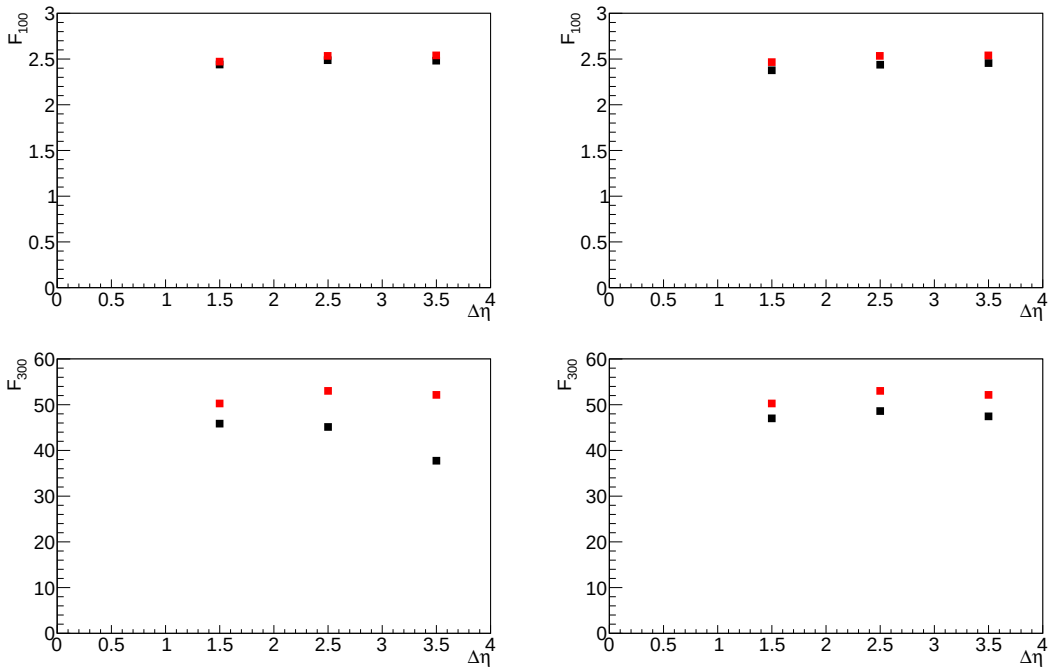

Figure 6: Comparison of values calculated from the truth level (red points) and unfolded from the reconstructed level (black points) for factorial moments F_{100} and F_{300}. Unfolding is done using a polynomial of degree 6 (left) and an exponential function e^{ax^2+bx+c} (right).

Figures 6 and 7 show tests of the HBOM procedure for two factorial moments (F_{100} and F_{300}). The factorial moments are presented as a function of the distance between the centres of the left and right bin. Values in the first figure are calculated with standard track selection cuts. Both functions are shown to unfold true values of the factorial moments incorrectly. The difference between the true and unfolded values for the polynomial is growing with larger distance between left and right bin, while values obtained

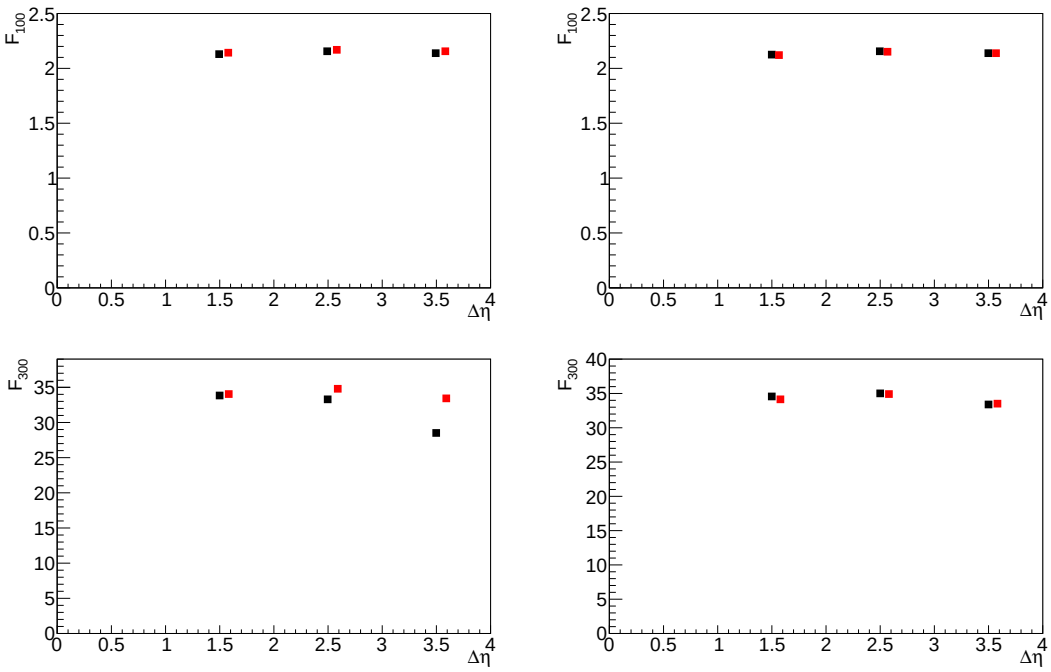

Figure 7: Comparison of values calculated from the truth level (red points) and unfolded from the reconstructed level (black points) for factorial moments F_{100} and F_{300} with the p_T cut changed from 100 MeV to 200 MeV. Unfolding is done using a polynomial of degree 6 (left) and an exponential function e^{ax^2+bx+c} (right). Points representing the truth level are shifted for better visibility.

from extrapolating the exponential function are systematically shifted with respect to the truth level. In the second figure the p_T cut is increased to 200 MeV because of a higher tracking efficiency in this p_T range. With this change the polynomial still fails to correct the measurements, but the exponential is working correctly. In further analysis the exponential e^{ax^2+bx+c} is used with an increased p_T cut to unfold data.

6 Statistical and systematic uncertainties

Three main sources of uncertainties are studied: statistical uncertainties of factorial moments and the tracking efficiency as well as the p_T resolution. An overall uncertainty is obtained as the square root of the sum of squared uncertainties from all sources. Figure 9 shows measured values of all factorial moments together with their total uncertainties.

6.1 Statistical uncertainty

Statistical uncertainties of the factorial moments are obtained by propagating errors coming from the fitting procedure of the HBOM method. The fitted function f has the following form:

$$f = e^{ax^2+bx+c} + d \tag{11}$$

The statistical error of a factorial moment F is then calculated as:

$$\Delta F = \sqrt{\left(\frac{\partial f}{\partial a}\Delta a\right)^2 + \left(\frac{\partial f}{\partial b}\Delta b\right)^2 + \left(\frac{\partial f}{\partial c}\Delta c\right)^2 + \left(\frac{\partial f}{\partial d}\Delta d\right)^2} \tag{12}$$

with derivatives taken at $x = -1$, to where f is extrapolated.

6.2 Efficiency uncertainty

Statistical errors of tracking efficiency, secondaries and fakes ratios are connected with llimited statistics of the Monte Carlo sample. To evaluate the influence of these uncertainties, the measurement of factorial moments is repeated with efficiency increased and decreased by these errors. Results of this procedure are upper and lower limits on each factorial moment connected with efficiency uncertainties.

6.3 Transversal momentum resolution

Systematic uncertainty is connected with a finite p_T resolution of the detector. The resolution is calculated using the Monte Carlo sample as the ratio:

$$res = \frac{|p_T^{truth} - p_T^{reco}|}{p_T^{reco}} \tag{13}$$

where p_T^{reco} is the transversal momentum of a reconstructed track and p_T^{truth} is the transversal momentum of the truth level particle matched with this track.
In Figure 8 one can see that the resolution is about 3.5% near the 200 MeV cut. The p_T cut is changed by this value up and down and factorial moments are calculated again. Similarly to the efficiency uncertainty, one gets upper and lower limits connected with finite p_T resolution on the measured quantities.

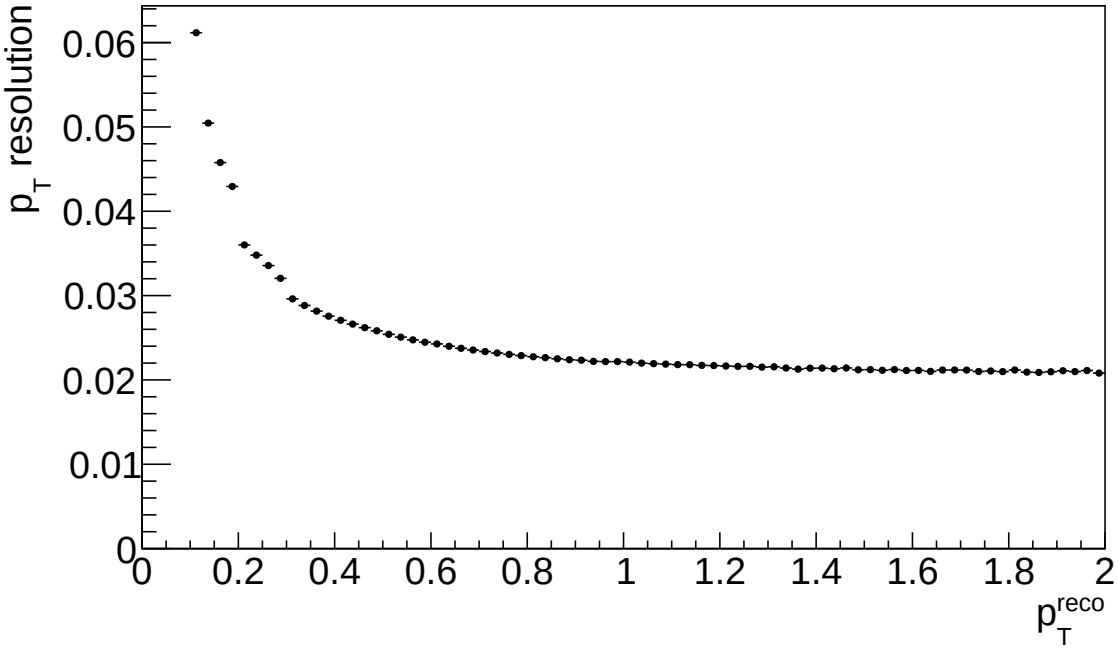

Figure 8: Reconstructed track p_T resolution as a function of p_T^{reco}.

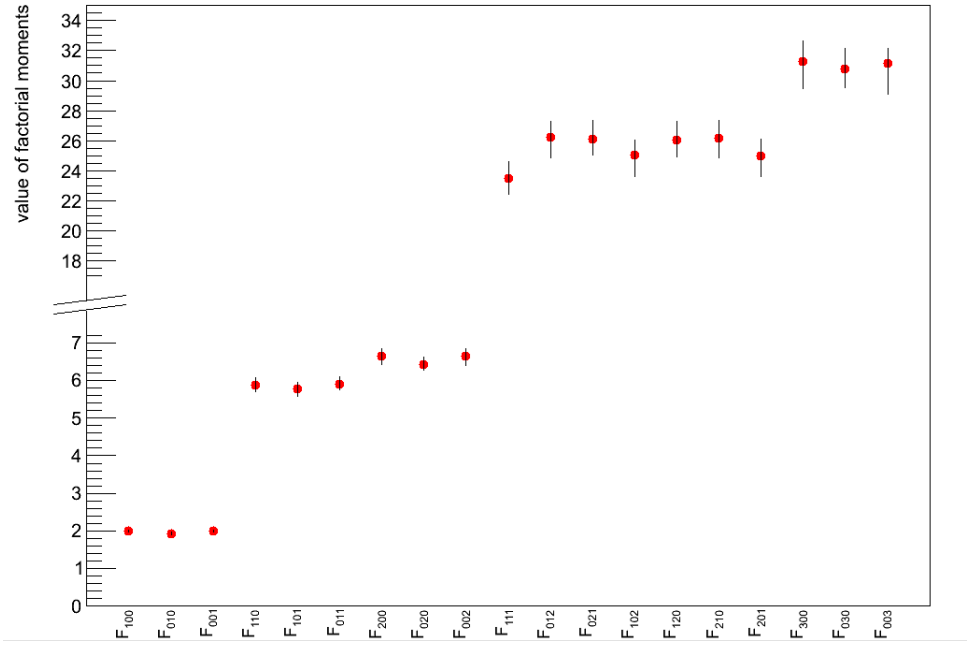

Figure 9: Measured values of 19 factorial moments up to rank three with their total uncertainties.

7 Results

To compare factorial moments obtained from data with models the following pseudorapidity bins are chosen:

$$\begin{gathered} \text{left: } -2 < \eta < -1.5 \\ \text{central: } -0.25 < \eta < 0.25 \\ \text{right: } 1.5 < \eta < 2 \end{gathered}$$

To measure long range correlations, bins with the biggest possible distance between them are needed. The distance between the chosen bins is the largest, for which the HBOM method should be working correctly (tracking efficiency in the left and right bin is higher than 60% and is decreasing rapidly for $|\eta| > 2$).

7.1 One source model

For comparison of data with a one source model, the factorial moments F_{100}, F_{010}, F_{001}, F_{002}, F_{003} are chosen to express parameters of the model described by (4). Then the rest of the factorial moments is calculated according to these equations. Figure 10 shows factorial moments obtained from data and model. Data values are systematically shifted with respect to the model, which indicates that a one source model seems to be disfavoured in pp collisions.

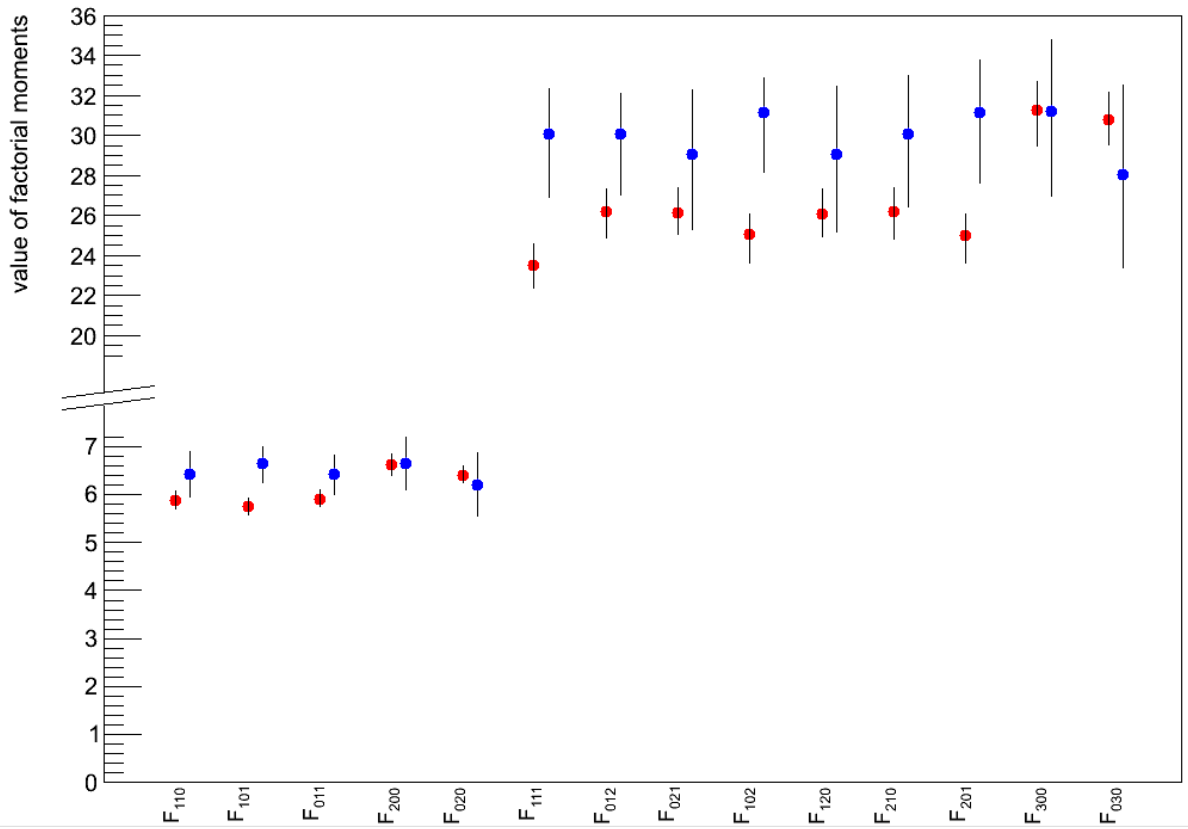

Figure 10: Comparison between factorial moments calculated from data (red points) and a model with one source (blue points). Points are shifted for better visibility.

7.2 Model with two sources

The equations in a two source model (6) are not as easy to solve as the ones in a model with one source. In this case the basic idea is to carry out a simultaneous fit of 10 parameters to all 19 equations using the MINUIT package. Uncertainties are obtained by propagating errors from the fitting procedure. Figure 11 shows factorial moments obtained from data and model. Data are in good agreement with a two source model.

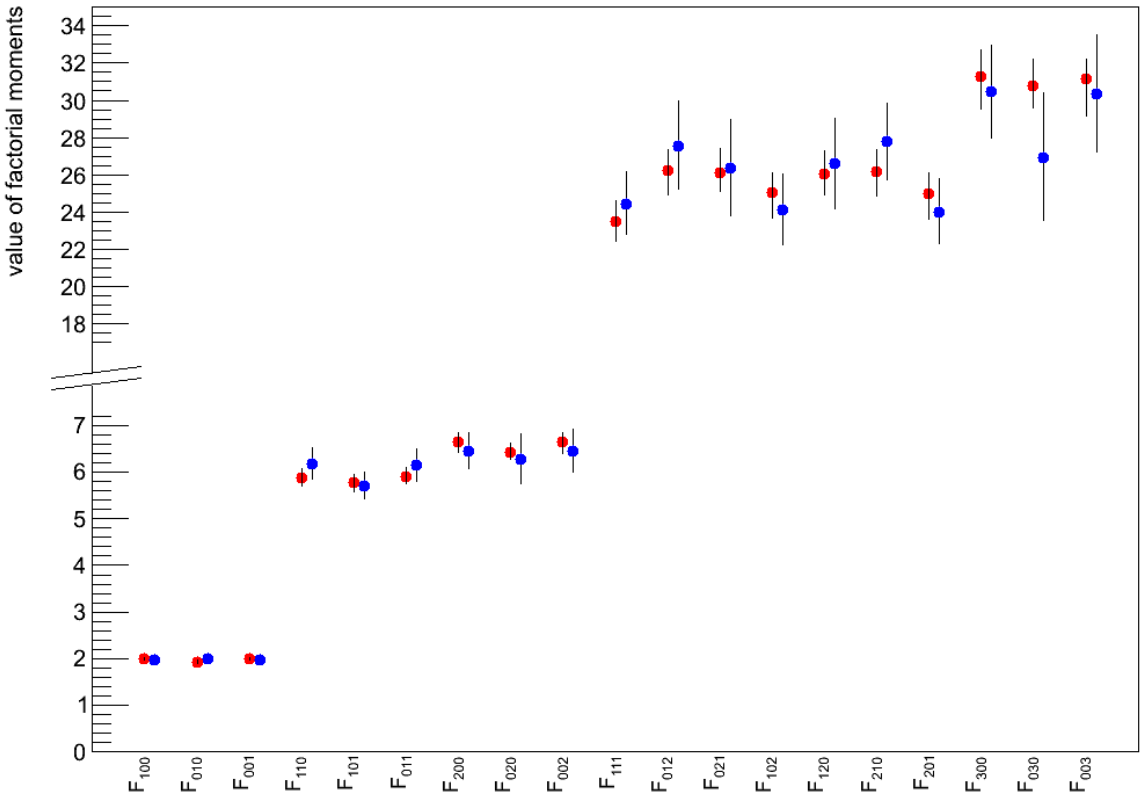

Figure 11: Comparison between factorial moments calculated from data (red points) and a model with two sources (blue points). Points are shifted for better visibility.

Values of all factorial moments measured from data and calculated from the one and two source models can be found in Appendix A.

8 High multiplicity *pp* collisions

A plan for the future is to extend the measurements presented in this report to high multiplicity *pp* collisions at the same center of mass energy ($\sqrt{s} = 2.76$ TeV). First preparations for such an analysis have been made. The dataset for high multiplicity measurements was collected in 2013 during runs 219257, 219263, 219296, 219305, 219322 and 219364 at the ATLAS detector. High multiplicity events are selected by a high multiplicity trigger (HMT) - EF_mbSpTrkVtxMh_pp_trk50_L1TE0_pileupSup which requires at least 50 reconstructed tracks with p_T over 400 MeV.
A Monte Carlo sample is not available for these data, so a request for production of a sample has to be made. For this request, cuts for a ChargedTracksFilter, which will pass generated events to simulation at the detector level, are estimated using the minimum bias Monte Carlo sample. As signal, which should be passed, we define all events which

contain at least 50 reconstructed tracks satisfying the condition $p_T > 400$ MeV. Table 4 summarizes the results of this analysis.

In addition, studies of the HMT efficiency are conducted. The efficiency of this trigger is calculated in two steps. The HMT efficiency is first evaluated with respect to the Level 1 trigger L1_TE0, by which the HMT is seeded:

$$\epsilon_{\text{HMT}} = \frac{\#\text{ events passing}(\texttt{L1\_TE0} \wedge \texttt{HMT} \wedge \text{offline selection})}{\#\text{ events passing}(\texttt{L1\_TE0} \wedge \text{offline selection})} \tag{14}$$

Then the efficiency of this Level 1 trigger is calculated with respect to the minimum bias trigger mbSpTrk (which is known to have a 100% efficiency):

$$\epsilon_{\text{L1\_TE0}} = \frac{\#\text{ events passing}(\texttt{mbSpTrk} \wedge \texttt{L1\_TE0} \wedge \text{offline selection})}{\#\text{ events passing}(\texttt{mbSpTrk} \wedge \text{offline selection})} \tag{15}$$

In both (12) and (13) offline selection denotes events with at least two tracks satisfying the following requirements:

- track $p_T > 100$ MeV,
- track pseudorapidity $|\eta| < 2.5$,
- at least one Pixel hit,
- at least two SCT hits for tracks with 100 MeV $< p_T <$ 200 MeV,
- at least four SCT hits for tracks with 200 MeV $< p_T <$ 300 MeV,
- at least six SCT hits for tracks with $p_T > 300$ MeV,
- at least one B-Layer hit when expected,
- TMath::Prob(χ^2,DoF) > 0.01 for tracks with $p_T > 10$ GeV,
- $|d_0^{PV}| < 1.5$ mm,
- $|z_0^{PV} \sin(\theta)| < 1.5$ mm.

Figures 12 and 13 show both steps of efficiency calculation as a function of track multiplicity for tracks with $p_T > 400$ MeV. The HMT efficiency reaches 100% for about 10 tracks above the designed threshold (50 tracks), but the efficiency of the L1_TE0 trigger is not reaching 100% for multiplicities lower than 110 tracks. Therefore data triggered by the chosen HMT cannot be used in the analysis, because propagating errors connected with the trigger efficiency would give very large uncertainties of the measured values.

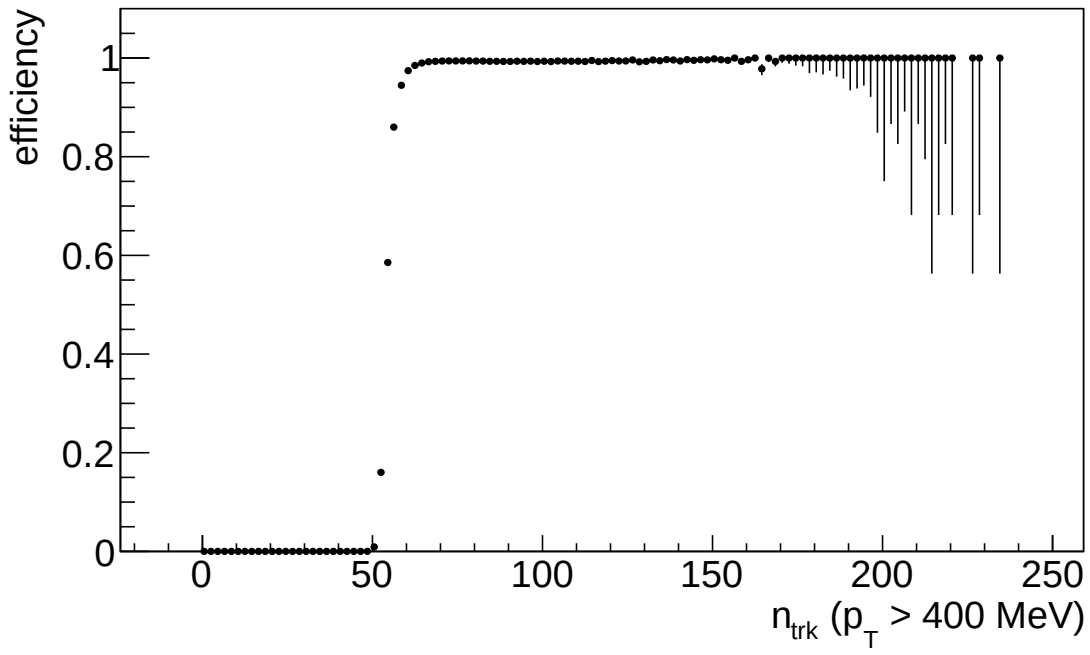

Figure 12: Efficiency of HMT as a function of the number of tracks with $p_T > 400$ MeV. A definition of the efficiency can be found in the text.

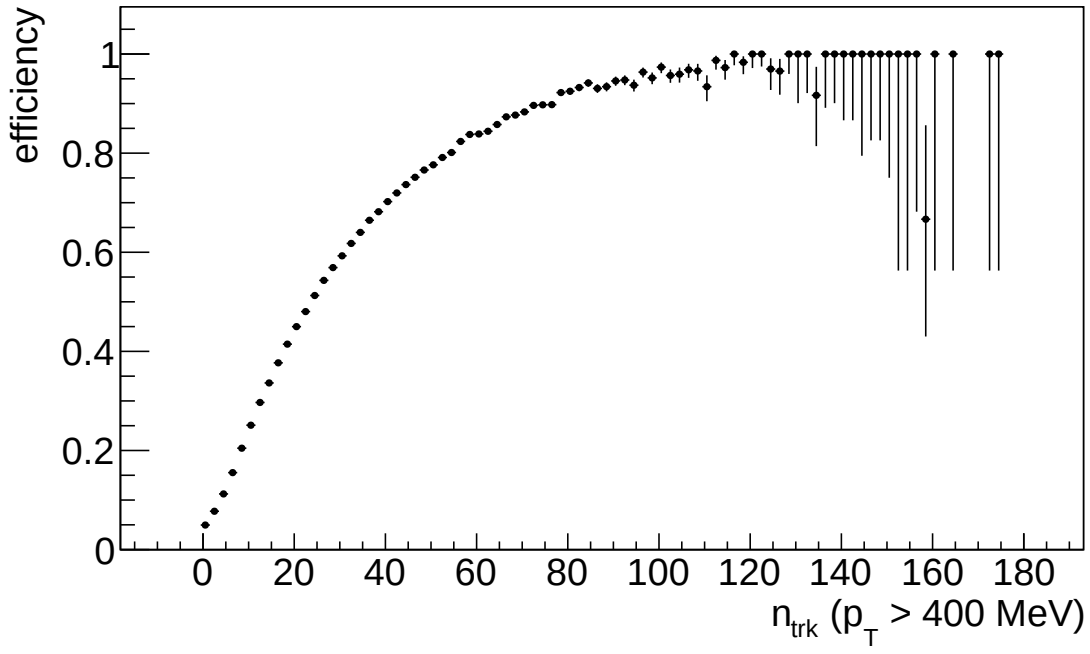

Figure 13: Efficiency of L1_TE0 as a function of the number of tracks with $p_T > 400$ MeV. A definition of the efficiency can be found in the text.

n_{part} \ p_T	370 [MeV]	380 [MeV]	390 [MeV]	400 [MeV]	410 [MeV]
45	100 5.47	100 6.05	100 6.70	100 7.42	100 8.25
46	100 6.12	100 6.78	100 7.53	100 8.38	100 9.35
47	100 6.85	100 7.61	100 8.47	100 9.47	100 10.6
48	100 7.68	100 8.57	100 9.56	100 10.71	100 12.03
49	100 8.62	100 9.65	100 10.82	100 12.14	100 13.68
50	100 9.70	100 10.88	100 12.24	100 13.81	100 15.6
51	100 10.93	100 12.29	100 13.88	100 15.68	100 17.79
52	100 12.34	100 13.93	100 15.76	99.99 17.88	99.96 20.38
53	100 13.93	100 15.78	100 17.93	99.97 20.45	99.84 23.28
54	99.99 15.75	99.97 17.89	99.97 20.4	99.88 23.25	99.63 25.56
55	99.97 17.89	99.91 20.36	99.84 23.25	99.68 26.61	99.22 30.43
56	99.87 20.29	99.78 23.12	99.64 26.5	99.3 30.37	98.47 34.62
57	99.73 23.02	99.61 26.35	99.31 30.23	98.65 34.56	97.18 39.34
58	99.52 26.13	99.15 29.95	98.62 34.44	97.47 39.31	95.4 44.61
59	99.07 29.76	98.45 34.11	97.49 39.01	95.67 44.24	92.67 50.09

Table 4: Analysis of cuts for a ChargedTracksFilter. Results are shown for different cuts on the number of particles at the truth level (n_{part}) with a certain p_T. The upper value in each cell shows which percentage of the signal is passed, while the lower value describes the percentage of the signal in the sample of all passed events.

9 Conclusions

Measurements of charged particle correlations in three bins of pseudorapidity in pp collisions at a center of mass energy $\sqrt{s} = 2.76$ TeV from the ATLAS experiment are presented in this report. Factorial moments are measured for particles with a transversal momentum above 200 MeV.

The results are compared with predictions of hydrodynamical models with one or two particle-emitting sources. The one source model seems to be disfavoured by the data, while the two source model is in good agreement with the data.

Preparations for a similar analysis with high multiplicity collisions are presented. The measurement cannot be continued because of a low efficiency for the chosen high multiplicity trigger.

References

[1] A. Białas, K. Zalewski, *Hydrodynamics of long range correlations*, Phys. Lett. **B 698** (2011) 416.

[2] A. Białas, K. Zalewski, *Hidden assymetry and forward-backward correlations*, Phys. Rev. **C 82** (2010) 034911.

[3] A. Białas, K. Zalewski, *Multibin long range correlations*, Nucl. Phys. **A 860** (2011) 56.

[4] https://twiki.cern.ch/twiki/bin/viewauth/AtlasProtected/MinimumBiasEventsSelection

[5] J. Monk, C. Oropeza-Barrera, *The HBOM method for unfolding detector effects*, Nucl. Instrum. Meth. **A 701** (2013) 17.

A Appendix

factorial moment	measured value	Δ_{stat}	Δ_{eff}^{up}	Δ_{eff}^{down}	$\Delta_{p_T}^{up}$	$\Delta_{p_T}^{down}$
F_{100}	1.977	0.005	0.011	0.011	0.033	0.035
F_{010}	1.909	0.044	0.008	0.006	0.032	0.028
F_{001}	1.977	0.005	0.012	0.008	0.034	0.033
F_{110}	5.868	0.011	0.068	0.056	0.186	0.181
F_{101}	5.749	0.012	0.06	0.058	0.177	0.199
F_{011}	5.871	0.011	0.059	0.042	0.189	0.173
F_{200}	6.632	0.016	0.071	0.088	0.201	0.233
F_{020}	6.395	0.022	0.059	0.04	0.198	0.173
F_{002}	6.628	0.016	0.069	0.078	0.184	0.245
F_{111}	23.471	0.073	0.396	0.353	1.039	1.108
F_{012}	26.218	0.099	0.324	0.449	1.047	1.334
F_{021}	26.126	0.095	0.39	0.275	1.182	1.082
F_{102}	25.034	0.096	0.307	0.455	0.968	1.413
F_{120}	26.066	0.094	0.502	0.3	1.130	1.171
F_{210}	26.193	0.098	0.461	0.43	1.072	1.336
F_{201}	25.019	0.097	0.344	0.507	1.018	1.356
F_{300}	31.256	0.163	0.492	0.744	1.316	1.658
F_{030}	30.755	0.144	0.488	0.267	1.318	1.240
F_{003}	31.144	0.163	0.187	0.722	0.979	1.976

Table 5: Measured values of all factorial moments up to rank three in pseudorapidity bins $|\eta| < 0.25$ and $1.5 < |\eta| < 2$ together with statistical and systematical uncertainties.

factorial moment	predicted value	Δ^{up}	Δ^{down}
F_{110}	6.40	0.47	0.49
F_{101}	6.63	0.35	0.41
F_{011}	6.4	0.41	0.44
F_{200}	6.63	0.54	0.57
F_{020}	6.18	0.67	0.66
F_{111}	30.08	2.25	3.27
F_{012}	30.07	1.99	3.10
F_{021}	29.03	3.19	3.82
F_{102}	31.15	1.72	3.06
F_{120}	29.04	3.35	3.95
F_{210}	30.09	2.91	3.74
F_{201}	31.16	2.57	3.58
F_{300}	31.17	3.55	4.32
F_{030}	28.03	4.43	4.72

Table 6: Values of factorial moments in pseudorapidity bins $|\eta| < 0.25$ and $1.5 < |\eta| < 2$ predicted by the one source model together with propagated uncertainties.

factorial moment	fitted value	Δ
F_{100}	1.95	0.07
F_{010}	1.98	0.09
F_{001}	1.96	0.08
F_{110}	6.16	0.34
F_{101}	5.67	0.29
F_{011}	6.13	0.35
F_{200}	6.42	0.4
F_{020}	6.24	0.55
F_{002}	6.41	0.46
F_{111}	24.44	1.7
F_{012}	27.55	2.4
F_{021}	26.36	2.61
F_{102}	24.1	1.94
F_{120}	26.58	2.45
F_{210}	27.77	2.07
F_{201}	24.01	1.77
F_{300}	30.44	2.52
F_{030}	26.9	3.46
F_{003}	30.33	3.16

Table 7: Values of factorial moments in pseudorapidity bins $|\eta| < 0.25$ and $1.5 < |\eta| < 2$ fitted from the two source model together with propagated uncertainties.